

AN ADAPTIVE INVERSE ITERATION FEM FOR THE INHOMOGENEOUS DIELECTRIC WAVEGUIDES*

Jianhua Yuan

(School of Science, Beijing University of Posts and Telecommunications, Beijing 100876, China

Email: yuan_bupt@yahoo.com.cn)

Abstract

We introduce an adaptive finite element method for computing electromagnetic guided waves in a closed, inhomogeneous, pillared three-dimensional waveguide at a given frequency based on the inverse iteration method. The problem is formulated as a generalized eigenvalue problems. By modifying the exact inverse iteration algorithm for the eigenvalue problem, we design a new adaptive inverse iteration finite element algorithm. Adaptive finite element methods based on a posteriori error estimate are known to be successful in resolving singularities of eigenfunctions which deteriorate the finite element convergence. We construct a posteriori error estimator for the electromagnetic guided waves problem. Numerical results are reported to illustrate the quasi-optimal performance of our adaptive inverse iteration finite element method.

Mathematics subject classification: 65N30, 65N25, 78A50.

Key words: Waveguides, Eigenvalue Problem, Inverse Iteration Algorithm, Adaptive Finite Element Method.

1. Introduction

In this paper we consider a closed waveguide defined by a right cylinder with cross section Ω , a bounded, Lipschitz, simply connected polyhedral domain in \mathbf{R}^2 . The waveguide is filled with an inhomogeneous media whose electromagnetic properties are described by the real-valued functions ε and μ . We assume that the magnetic permeability $\mu = \mu_0$, the magnetic permeability in vacuum, and the dielectric permittivity ε is piecewise constant and has no variation along the waveguide. More precisely, let $\Omega_1 \subset \Omega$ be an open domain, $\Omega_2 = \Omega \setminus \bar{\Omega}_1$. We assume that

$$\varepsilon(x) = \begin{cases} \varepsilon_1 \varepsilon_0 & \text{in } \Omega_1, \\ \varepsilon_2 \varepsilon_0 & \text{in } \Omega_2, \end{cases}$$

where ε_0 is the dielectric permittivity in vacuum.

The waveguide problem is to find solutions to the Maxwell equations which are of the general form

$$\begin{cases} \mathcal{E}(\mathbf{x}, x_3, t) = (\mathbf{E}(\mathbf{x}), E_3(\mathbf{x}))e^{i(\omega t - \beta x_3)}, \\ \mathcal{H}(\mathbf{x}, x_3, t) = (\mathbf{H}(\mathbf{x}), H_3(\mathbf{x}))e^{i(\omega t - \beta x_3)}, \end{cases} \quad (1.1)$$

where $\mathbf{x} = (x_1, x_2) \in \Omega$ and the x_3 -axis is along the waveguide, $\omega > 0$ is the angular frequency of the guided wave, β is the constant of propagation, \mathbf{E} and \mathbf{H} are electric and magnetic field components in the plane of the cross section, and E_3 and H_3 are electric and magnetic components along the waveguide.

* Received November 9, 2005; final revised May 24, 2006; accepted June 29, 2006.

With expression (1.1), the second-order three-dimensional Maxwell equations expressed in terms of the electric field (\mathbf{E}, E_3) reduce to the following two-dimensional equations (cf. e.g. [7, 19, 22]):

$$\begin{cases} \nabla \times (\nabla \times \mathbf{E}) - i\beta \nabla E_3 - (\omega^2 \varepsilon_0 \mu_0) \varepsilon \mathbf{E} + \beta^2 \mathbf{E} = 0, & \text{in } \Omega; \\ -\nabla \cdot (\nabla E_3) - (\omega^2 \varepsilon_0 \mu_0) \varepsilon E_3 - i\beta \nabla \cdot \mathbf{E} = 0, & \text{in } \Omega; \\ \nabla \cdot (\varepsilon \mathbf{E}) - i\beta \varepsilon E_3 = 0, & \text{in } \Omega. \end{cases} \quad (1.2)$$

For simplicity, perfect electric conductor boundary conditions are imposed:

$$\mathbf{E} \times \mathbf{n} = 0, \quad E_3 = 0 \quad \text{on } \partial\Omega, \quad (1.3)$$

where \mathbf{n} is the unit outer normal to $\partial\Omega$.

Advances in various branches of photonics technologies have established the need for the development of numerical and approximate methods for the analysis of a wide range of waveguide structures that are not amenable to exact analytical studies ([8, 12, 14]). Since no sources are given, (1.2)–(1.3) is an eigenvalue problem. Either ω or β is assumed to be known, and the goal is to find all possible pairs which consist of the other missing constant β or ω and the corresponding field (\mathbf{E}, E_3) . Probably the first finite element analysis of the waveguide problems was developed in the 1960s ([14]). Current finite element methods for computing waveguide have been developed by using varied finite element technologies (see, e.g., [4, 7, 8, 14, 15, 19]). In [7], we investigated the finite element methods over the uniformly refined meshes for this problem in the more physically relevant case, when ω is given, but β is unknown. A similar finite element analysis was recently studied in [19].

For the simplest geometries, the finite element methods reported in [7] and [19] are quasi-optimal. But the structure of the more interesting waveguides encountered in extensive applications is always very complex. With the complex structure, the eigenfunctions of the eigenvalue problem usually display singularities which deteriorate the finite element convergence if uniform mesh refinements are used. We show one such situation in [7] that points to the serious problem. However, adaptive finite element methods based on a posteriori error estimates are known to be successful in resolving this difficulty [5, 20]. Introducing the adaptive finite element method for computing electromagnetic guided waves problem at a given frequency is our main work in this paper. Compared with the traditional adaptive finite element methods for eigenvalue problems, our method is simpler, since the a posteriori error estimators are easily obtained.

In this paper, we will discuss the adaptive finite element algorithm for computing electromagnetic guided waves in a closed, inhomogeneous, pillared three-dimensional waveguide at a given frequency based on the finite element formulation given by [7] and [19] (see [22] for more details).

Let $\mathbb{X} = H_0(\mathbf{curl}; \Omega) \times H_0^1(\Omega)$ equipped with the norm

$$\|(\mathbf{V}, q)\|_{\mathbb{X}} = \|\mathbf{V}\|_{\mathbf{curl}, \Omega} + \|q\|_{H^1(\Omega)} \quad \forall (\mathbf{V}, q) \in \mathbb{X}.$$

Here,

$$\|\mathbf{V}\|_{\mathbf{curl}, \Omega} = (\|\nabla \times \mathbf{V}\|_{L^2(\Omega)}^2 + \|\mathbf{V}\|_{L^2(\Omega)}^2)^{1/2}$$

is the norm of the space $H(\mathbf{curl}; \Omega)$ which is defined as the collection of all functions \mathbf{V} in $L^2(\Omega)$ such that $\|\mathbf{V}\|_{\mathbf{curl}, \Omega} < \infty$. $H_0(\mathbf{curl}; \Omega)$ consists of functions \mathbf{V} in $H(\mathbf{curl}; \Omega)$ whose tangential component $\mathbf{V} \times \mathbf{n}$ vanishes on the boundary $\partial\Omega$.

Let $E_3^{\text{new}} = i\beta E_3$. To save the notation, E_3 will represent E_3^{new} for the remainder of this paper. Similar to in [7], [19] and [22], our goal is to solve the following variational problem for

a given frequency $\omega > 0$: Find pairs $(\lambda, (\mathbf{E}, E_3)) \in \mathbb{C} \times \mathbb{X}$, such that

$$\mathbf{a}((\mathbf{E}, E_3), (\mathbf{V}, q)) = \lambda \mathbf{b}((\mathbf{E}, E_3), (\mathbf{V}, q)) \quad \forall (\mathbf{V}, q) \in \mathbb{X}. \quad (1.4)$$

For any $(\mathbf{U}, p), (\mathbf{V}, q) \in \mathbb{X}$, the bilinear forms $\mathbf{a} : \mathbb{X} \times \mathbb{X} \rightarrow \mathbb{C}$ and $\mathbf{b} : \mathbb{X} \times \mathbb{X} \rightarrow \mathbb{C}$ are defined as follows:

$$\begin{aligned} \mathbf{a}((\mathbf{U}, p), (\mathbf{V}, q)) &= \langle \nabla \times \mathbf{U}, \nabla \times \mathbf{V} \rangle - \langle k_0^2 \varepsilon \mathbf{U}, \mathbf{V} \rangle - \langle \nabla p, \mathbf{V} \rangle \\ &\quad + k_0^2 (\langle \varepsilon \mathbf{U}, \nabla q \rangle + \langle \varepsilon p, q \rangle), \end{aligned} \quad (1.5)$$

$$\mathbf{b}((\mathbf{U}, p), (\mathbf{V}, q)) = \langle -\mathbf{U}, \mathbf{V} \rangle, \quad (1.6)$$

where $\lambda = \beta^2$, $k_0^2 = \omega^2 \varepsilon_0 \mu_0$.

From the theory of variational eigenvalue problems [1], the existence of solutions to (1.4) is equivalent to the following continuous inf-sup condition and was proved in [19]. There is a similar theorem in [7].

Theorem 1.1. *With the assumption on ω in (3.15) of [19], the continuous form $\mathbf{a}(\cdot, \cdot)$ satisfies the following conditions:*

There exists $\alpha > 0$ such that for any $(\mathbf{U}, p) \in \mathbb{X}$,

$$\sup_{(\mathbf{V}, q) \in \mathbb{X}} \frac{|\mathbf{a}((\mathbf{U}, p), (\mathbf{V}, q))|}{\|(\mathbf{V}, q)\|_{\mathbb{X}}} \geq \alpha \|(\mathbf{U}, p)\|_{\mathbb{X}}, \quad (1.7)$$

and for any $(\mathbf{V}, q) \in \mathbb{X}$, $(\mathbf{V}, q) \neq 0$,

$$\sup_{(\mathbf{U}, p) \in \mathbb{X}} |\mathbf{a}((\mathbf{U}, p), (\mathbf{V}, q))| > 0. \quad (1.8)$$

Let \mathcal{M}_h be a shape regular triangulation of Ω . For any $K \in \mathcal{M}_h$, we denote by h_K its diameter, and set $h = \max_{K \in \mathcal{M}_h} h_K$. Denote $\mathbb{X}_h = \mathbf{W}_h \times Q_h$, where $Q_h \subset H_0^1(\Omega)$ is the standard conforming linear finite element space, and $\mathbf{W}_h \subset H_0(\mathbf{curl}; \Omega)$ be the finite element space of the lowest order $H(\mathbf{curl}; \Omega)$ conforming edge element:

$$\begin{aligned} \mathbf{W}_h = \{ \mathbf{V}_h \in H_0(\mathbf{curl}; \Omega) : \mathbf{V}_h|_K &= (a_K - c_K x_2, b_K + c_K x_1)^T, \\ &\text{where } a_K, b_K, c_K \in \mathbf{R}, K \in \mathcal{M}_h \}. \end{aligned}$$

The finite element approximation of the variationally posed eigenvalue problem (1.4) is as follow: Find all pairs $(\lambda_h, (\mathbf{E}_h, E_{3h})) \in \mathbb{C} \times \mathbb{X}_h$, such that

$$\mathbf{a}((\mathbf{E}_h, E_{3h}), (\mathbf{V}_h, q_h)) = \lambda_h \mathbf{b}((\mathbf{E}_h, E_{3h}), (\mathbf{V}_h, q_h)), \quad \forall (\mathbf{V}_h, q_h) \in \mathbb{X}_h. \quad (1.9)$$

Similarly, the discrete inf-sup condition on $\mathbf{a}(\cdot, \cdot)$ which is studied in Theorem 5 of [19] ensures the existence of solutions to the discrete problem (1.9).

The outline of the remainder of this paper is as follows. In section 2, we shall construct an new adaptive method for the eigenvalue problems, and our method is based on the inverse iteration algorithm and is named adaptive inverse iteration finite element algorithm (AIIFEA). For the electromagnetic guided waves problem, in section 3, we construct an a posteriori error estimator and give a full adaptive procedure. We also report several numerical experiments in the last section to illustrate the performance of the method studied in this paper.

2. Adaptive Inverse Iteration Finite Element Algorithm

To avoid complicated expressions, we consider the following simple eigenvalue problem: find pairs $(\lambda, \mathbf{U}) \in \mathbb{C} \times \mathbb{X}$ such that

$$\mathbf{F}(\mathbf{U}, \mathbf{V}) = \lambda \mathbf{G}(\mathbf{U}, \mathbf{V}), \quad \forall \mathbf{V} \in \mathbb{X}, \quad (2.1)$$

where \mathbb{X} is a Hilbert space, $\mathbf{F}(\cdot, \cdot)$ and $\mathbf{G}(\cdot, \cdot) : \mathbb{X} \times \mathbb{X} \rightarrow \mathbb{C}$ are bilinear forms.

We start this section by describing the standard exact inverse iteration algorithm (EIIA) in infinite dimensions as an iteration to solve (2.1).

Exact Inverse Iteration Algorithm (EIIA)

Choose parameters $\epsilon_r > 0$, $\kappa_0 > 0$; set $j = 0$.

1. Set $\tilde{\mathbf{U}}_0 \in \mathbb{X}$ satisfies $\mathbf{G}(\tilde{\mathbf{U}}_0, \tilde{\mathbf{U}}_0) = 1$.
2. $j = j + 1$.
3. Compute $\tilde{\mathbf{U}}_j^* \in \mathbb{X}$ which is the solution of the variational problem

$$\mathbf{F}(\tilde{\mathbf{U}}_j^*, \mathbf{V}) = \mathbf{G}(\tilde{\mathbf{U}}_{j-1}, \mathbf{V}), \quad \forall \mathbf{V} \in \mathbb{X}. \quad (2.2)$$

4. $\kappa_j = \frac{\mathbf{F}(\tilde{\mathbf{U}}_j^*, \tilde{\mathbf{U}}_j^*)}{\mathbf{G}(\tilde{\mathbf{U}}_j^*, \tilde{\mathbf{U}}_j^*)}$, $\tilde{\mathbf{U}}_j = \frac{\tilde{\mathbf{U}}_j^*}{(\mathbf{G}(\tilde{\mathbf{U}}_j^*, \tilde{\mathbf{U}}_j^*))^{1/2}}$.
5. If $|(\kappa_j - \kappa_{j-1})/\kappa_j| < \epsilon_r$ goto (6);
else goto (2).
6. Output κ_j , $\tilde{\mathbf{U}}_j$.

Remark 2.1. *Generally, the inverse iteration algorithm is used to compute the eigenvalue with the least modulus and the corresponding eigenvector. If we want to obtain other eigenvalues and the corresponding eigenvectors, we can use the shift inverse iteration finite element algorithm. For more details, please see [22].*

Our adaptive inverse iteration finite element algorithm is motivated by the Adaptive UZAWA Finite Element Method for the Stokes problem that was investigated by Bansch, Morin and Nocketto (see [2]). We construct an adaptive inverse iteration finite element algorithm based on EIIA that is different from the traditional adaptive finite element method for the eigenvalue problems. Our adaptive algorithm consists of an inexact inner adaptive procedure ADAPTIVE for the discrete variational problem, in place of the computation of (2.2).

To approximate (λ, \mathbf{U}) , we consider a sequence of triangulations $\{\mathcal{M}_{j,h}\}_{j=0,1,2,3,\dots}$ of the shape regular triangulation of Ω . Let $\mathbb{X}_{j,h} \subset \mathbb{X}$ be the linear finite element subspace of \mathbb{X} over $\mathcal{M}_{j,h}$, where j is the iteration number. In this section, to be simple, we omit the subscript h , $\{\mathcal{M}_j\}$ will be the j -th shape regular triangulation of Ω , and \mathbb{X}_j the linear finite element subspace of the j -th iteration.

Given $\tilde{\mathbf{U}}_{j-1} \in \mathbb{X}_{j-1}$ for $j \geq 1$, let \mathbf{U}_j denote the exact solution of the following variational problem:

$$\mathbf{U}_j \in \mathbb{X} : \quad \mathbf{F}(\mathbf{U}_j, \mathbf{V}) = \mathbf{G}(\tilde{\mathbf{U}}_{j-1}, \mathbf{V}), \quad \forall \mathbf{V} \in \mathbb{X}.$$

If $\epsilon_j > 0$ stands for an adjustable error tolerance, then in place of solving (2.2), the procedure ADAPTIVE

$$(\tilde{\mathbf{U}}_j, \mathcal{M}_j) \leftarrow \text{ADAPTIVE}(\tilde{\mathbf{U}}_{j-1}, \mathcal{M}_{j-1}, \epsilon_j)$$

finds adaptively a refined mesh \mathcal{M}_j of \mathcal{M}_{j-1} and solves the discrete eigenvalue problem

$$\tilde{\mathbf{U}}_j \in \mathbb{X}_j : \quad \mathbf{F}(\tilde{\mathbf{U}}_j, \mathbf{V}_j) = \mathbf{G}(\tilde{\mathbf{U}}_{j-1}, \mathbf{V}_j), \quad \forall \mathbf{V}_j \in \mathbb{X}_j, \quad (2.3)$$

within the prescribed error bound

$$\|\mathbb{U}_j - \tilde{U}_j\|_{\mathbf{a}} \leq C\epsilon_j, \quad (2.4)$$

where $C > 0$ is independent of j .

Now, we give the adaptive inverse iteration finite element algorithm to solve the variational eigenvalue problem.

Adaptive Inverse Iteration Finite Element Algorithm(AIIFEA)

Choose parameters $\epsilon_r > 0$, $\epsilon_0 > 0$, $0 < \rho < 1$, κ_0 ; set $j = 0$.

1. Select any initial mesh \mathcal{M}_0 ; and let $\tilde{U}_0 \in \mathbb{X}_0$ satisfy $\mathbf{G}(\tilde{U}_0, \tilde{U}_0) = 1$.
2. Set $j = j + 1$, $\epsilon_j = \rho\epsilon_{j-1}$.
3. Compute $(\tilde{U}_j^*, \mathcal{M}_j)$, where

$$(\tilde{U}_j^*, \mathcal{M}_j) \leftarrow \text{ADAPTIVE}(\tilde{U}_{j-1}, \mathcal{M}_{j-1}, \epsilon_j).$$

4. $\kappa_j = \frac{\mathbf{F}(\tilde{U}_j^*, \tilde{U}_j^*)}{\mathbf{G}(\tilde{U}_j^*, \tilde{U}_j^*)}$, $\tilde{U}_j = \frac{\tilde{U}_j^*}{(\mathbf{G}(\tilde{U}_j^*, \tilde{U}_j^*))^{1/2}}$.
5. If $|(\kappa_j - \kappa_{j-1})/\kappa_j| < \epsilon_r$, goto (6);
else goto (2).
6. Output κ_j, \tilde{U}_j .

To avoid complicated notation and analysis, the AIIFEA given above just deals with the eigenvalue of least modulus. Similarly, there is a shift adaptive inverse iteration finite element algorithm to obtain the eigenvalue closest to the shift.

Our algorithm is a self-adaptive discretization method which has gained an enormous importance for the numerical solution of partial differential equations that arise from physical and technical applications. The key and main tool of the self-adaptive algorithm are error estimators and indicators which enable us to give global and local information on the error of the numerical solution using only the computed numerical solution and known data of the problem, and therefore ensure that the exact solution \mathbb{U}_j and the finite element solution \tilde{U}_j satisfy (2.4). The procedure ADAPTIVE of AIIFEA is a conventional adaptive algorithm, that is, it entails an inner loop of the form

SOLVE \rightarrow ESTIMATE \rightarrow REFINE

for the general elliptic problem (2.2). To achieve the error reduction of (2.4), we need upper and local lower a posteriori error bounds for (2.3) and a marking strategy. These issues are discussed in section 4.

When \mathbb{U}_j and \tilde{U}_j satisfy (2.4), our numerical experiments show that the Adaptive Inverse Iteration Finite Element Algorithm for the finite element eigenvalue problem can attain quasi-optimal performance. But the convergence analysis of this algorithm is also an open problem.

3. Posteriori Error Estimators

In this section we will derive an a posteriori error estimate for the vector $\tilde{U}_j = (\mathbf{E}_j, E_{3,j})$, $j \geq 1$, the solution of (2.3), and that ensures the error reduction of (2.4). We consider the following general variational problem that corresponds to problem (1.4):

Find $(\mathbf{E}, E_3) \in \mathbb{X}$, such that

$$\mathbf{a}((\mathbf{E}, E_3), (\mathbf{V}, q)) = \mathbf{b}((\mathbf{f}, 0), (\mathbf{V}, q)), \quad \forall (\mathbf{V}, q) \in \mathbb{X}, \quad (3.1)$$

where \mathbf{f} is an piecewise linear polynomial function.

Considering the j -th iteration of AIIFEA for the waveguide problem. \mathcal{M}_h is the j -th shape regular triangulation of Ω , $\mathbb{X}_h = \mathbf{W}_h \times Q_h$. Along with AIIFEA, we have $\mathbf{f} = -\mathbf{E}_{j-1,h}$. The corresponding finite element problem of (3.1) is as follows:

Find $(\mathbf{E}_h, E_{3,h}) \in \mathbb{X}_h$, such that

$$\mathbf{a}((\mathbf{E}_h, E_{3,h}), (\mathbf{V}_h, q_h)) = \mathbf{b}((\mathbf{f}, 0), (\mathbf{V}_h, q_h)), \quad \forall (\mathbf{V}_h, q_h) \in \mathbb{X}_h. \quad (3.2)$$

For establishing an a posteriori error estimate of (3.1) and (3.2), we firstly give a decomposition of the function space $H_0(\mathbf{curl}, \Omega)$ ([3, 11, 21]) and the property of the direct splitting as shown in following lemma. Lemma 3.1 may be proved by arguments similar to those in the proof of Theorem 2.3 of [21].

Lemma 3.1. *If $\Omega \in \mathbf{R}^2$ is a Lipschitz, bounded and simply connected domain, then for any $\mathbf{V} \in H_0(\mathbf{curl}, \Omega)$, there exist a constant C depending only on Ω , $\vec{\varphi} \in (H^1(\Omega))^2 \cap H_0(\mathbf{curl}, \Omega)$, and $\psi \in H_0^1(\Omega)$ such that*

$$\mathbf{V} = \vec{\varphi} + \nabla\psi$$

and

$$\|\vec{\varphi}\|_{H^1(\Omega)} \leq C\|\mathbf{V}\|_{H(\mathbf{curl}, \Omega)}, \quad (3.3)$$

$$\|\nabla\psi\|_{L^2(\Omega)} \leq C\|\mathbf{V}\|_{H(\mathbf{curl}, \Omega)}. \quad (3.4)$$

For $D \subseteq \Omega$, the set of vertices and edges in D are denoted by $\mathcal{N}_h(D)$ and $\mathcal{B}_h(D)$. For any $K \in \mathcal{M}_h$, $e \in \mathcal{B}_h(\Omega)$, we designate that

$$\begin{aligned} \mathfrak{S}(K) &= \cup\{K' \in \mathcal{M}_h, \quad (K' \cap K) \in (\mathcal{B}_h(\Omega) \cup \mathcal{N}_h(\Omega))\}, \\ \wp(e) &= \cup\{K \in \mathcal{M}_h, \quad \mathcal{N}_h(e) \cap \mathcal{N}_h(K) \neq \emptyset\}. \end{aligned}$$

We introduce a linear interpolation operator $\Theta_h : H_0(\mathbf{curl}, \Omega) \rightarrow \mathbf{W}_h$ which is defined by

$$\Theta_h \mathbf{V} = \Theta_h(\vec{\varphi} + \nabla\psi) = \Pi_h \vec{\varphi} + \nabla r_h \psi, \quad \forall \mathbf{V} \in H_0(\mathbf{curl}, \Omega).$$

where $\Pi_h : (H^1(\Omega))^2 \cap H_0(\mathbf{curl}, \Omega) \rightarrow \mathbf{W}_h$ is the two-dimensional edge element interpolation operator and $r_h : L^2(\Omega) \rightarrow Q_h$ is the Clément interpolation operator ([9, 18, 20]). In two dimensions, the edge element interpolation operator has the following properties (see [17, 23]):

Lemma 3.2. *There exists a constant C depending only on the mesh shape-regularity such that*

$$\begin{aligned} \|\vec{\varphi} - \Pi_h \vec{\varphi}\|_{[L^2(K)]^2} &\leq Ch_K \|\vec{\varphi}\|_{H(\mathbf{curl}, K)}, \quad \forall K \in \mathcal{M}_h, \\ \|\vec{\varphi} - \Pi_h \vec{\varphi}\|_{[L^2(e)]^2} &\leq Ch_e^{\frac{1}{2}} \|\vec{\varphi}\|_{H(\mathbf{curl}, \mathfrak{S}(K))}, \quad \forall e \in \mathcal{B}_h(K), K \in \mathcal{M}_h. \end{aligned}$$

and the Clément interpolation operator has the following properties (see Corollary 3.1 of [6]):

Lemma 3.3. *There exists a constant C depending only on the mesh shape-regularity such that*

$$\begin{aligned} \|\psi - r_h\psi\|_{L^2(K)} &\leq Ch_K \|\nabla\psi\|_{L^2(\mathfrak{S}(K))}, \quad \forall K \in \mathcal{M}_h, \\ \|\psi - r_h\psi\|_{L^2(e)} &\leq Ch_e^{\frac{1}{2}} \|\nabla\psi\|_{L^2(\wp(e))}, \quad \forall e \in \mathcal{B}_h(\Omega). \end{aligned}$$

Theorem 3.4. (Upper Bound) *Let $(\mathbf{E}, E_3) \in \mathbb{X}$, $(\mathbf{E}_h, E_{3,h}) \in \mathbb{X}_h$ be the solutions of problem (3.1) and (3.2), respectively. Then there exists a constant $C > 0$, depending only on the mesh shape-regularity such that the following a posteriori upper bound for the error holds:*

$$\|\mathbf{E} - \mathbf{E}_h\|_{H(\mathbf{curl}, \Omega)} + \|E_3 - E_{3,h}\|_{H^1(\Omega)} \leq C \left(\sum_{K \in \mathcal{M}_h} \eta(K)^2 \right)^{\frac{1}{2}},$$

where the local error indicators $\eta(K)$ are given by

$$\eta(K)^2 = (\eta_1(K))^2 + \sum_{e \in \partial K, e \notin \partial \Omega} \eta_1(e)^2, \quad (3.5)$$

with

$$\begin{aligned} \eta_1(K)^2 &= h_K^2 (\|\mathbf{f} + k_0^2 \varepsilon \mathbf{E}_h + \nabla E_{3,h}\|_{[L^2(K)]^2}^2 + \|\nabla \cdot (\mathbf{f} + k_0^2 \varepsilon \mathbf{E}_h + \nabla E_{3,h})\|_{L^2(K)}^2 \\ &\quad + \|k_0^2 (\nabla \cdot (\varepsilon \mathbf{E}_h) - \varepsilon E_{3,h})\|_{L^2(K)}^2) \end{aligned}$$

and

$$\eta_1(e)^2 = h_e (\|\mathbf{f} + k_0^2 \varepsilon \mathbf{E}_h + \nabla E_{3,h}\|_{L^2(e)}^2 + \|k_0^2 [\varepsilon \mathbf{E}_h] \cdot \mathbf{n}_e\|_{L^2(e)}^2),$$

where \mathbf{n}_e is the unit normal of the edge e , and the definition of the jump $[\cdot]$ is that for any function $J \in (L^2(\Omega))^2$ or $L^2(\Omega)$: $[J] = (J|_{K_1} - J|_{K_2})$.

Proof. Since $(\mathbf{E}, E_3) \in \mathbb{X}$ and $(\mathbf{E}_h, E_{3,h}) \in \mathbb{X}_h$ are the solutions of (3.1) and (3.2), respectively, we denote the total error by $(\mathbf{e}, e_3) := (\mathbf{E} - \mathbf{E}_h, E_3 - E_{3,h}) \in \mathbb{X}$. It is easy to see that for all $(\mathbf{V}, q) \in \mathbb{X}$ the error (\mathbf{e}, e_3) satisfies

$$\mathbf{a}((\mathbf{e}, e_3), (\mathbf{V}, q)) = \langle \mathbf{f}, \mathbf{V} - \Theta_h \mathbf{V} \rangle - \mathbf{a}((\mathbf{E}_h, E_{3,h}), (\mathbf{V} - \Theta_h \mathbf{V}, q - r_h q)).$$

From Lemma 3.1 and the definition of Θ_h , we have for any $\mathbf{V} \in H_0(\mathbf{curl}, \Omega)$,

$$\begin{aligned} \mathbf{V} &= \vec{\varphi} + \nabla\psi, \\ \Theta_h \mathbf{V} &= \Pi_h \vec{\varphi} + \nabla r_h \psi, \end{aligned}$$

where $\vec{\varphi} \in (H^1(\Omega))^2 \cap H_0(\mathbf{curl}, \Omega)$ and $\psi \in H_0^1(\Omega)$.

Then

$$\begin{aligned} &\mathbf{a}((\mathbf{e}, e_3), (\mathbf{V}, q)) \\ &= \langle \mathbf{f}, \mathbf{V} - \Theta_h \mathbf{V} \rangle - \mathbf{a}((\mathbf{E}_h, E_{3,h}), (\mathbf{V} - \Theta_h \mathbf{V}, q - r_h q)) \\ &= \langle \mathbf{f}, \vec{\varphi} - \Pi_h \vec{\varphi} + \nabla(\psi - r_h \psi) \rangle - \mathbf{a}((\mathbf{E}_h, E_{3,h}), (\vec{\varphi} - \Pi_h \vec{\varphi} + \nabla(\psi - r_h \psi), q - r_h q)) \\ &= \sum_{K \in \mathcal{M}_h} \langle \mathbf{f} + k_0^2 \varepsilon \mathbf{E}_h + \nabla E_{3,h}, \vec{\varphi} - \Pi_h \vec{\varphi} \rangle_K - \sum_{K \in \mathcal{M}_h} \langle \mathbf{curl} \mathbf{E}_h, \mathbf{curl}(\vec{\varphi} - \Pi_h \vec{\varphi}) \rangle_K \\ &\quad + \sum_{K \in \mathcal{M}_h} \langle \mathbf{f} + k_0^2 \varepsilon \mathbf{E}_h + \nabla E_{3,h}, \nabla(\psi - r_h \psi) \rangle_K - \sum_{K \in \mathcal{M}_h} k_0^2 \langle \varepsilon \mathbf{E}_h, \nabla(q - r_h q) \rangle_K \\ &\quad - \sum_{K \in \mathcal{M}_h} k_0^2 \langle \varepsilon E_{3,h}, q - r_h q \rangle_K \end{aligned}$$

$$\begin{aligned}
&= \sum_{K \in \mathcal{M}_h} (\langle \mathbf{f} + k_0^2 \varepsilon \mathbf{E}_h + \nabla E_{3,h}, \vec{\varphi} - \Pi_h \vec{\varphi} \rangle_K - \langle \nabla \cdot (\mathbf{f} + k_0^2 \varepsilon \mathbf{E}_h + \nabla E_{3,h}), \psi - r_h \psi \rangle_K) \\
&\quad + \sum_{e \in \mathcal{B}_h(\Omega), e \notin \partial\Omega} \int_e [(\mathbf{f} + k_0^2 \varepsilon \mathbf{E}_h + \nabla E_{3,h}) \cdot \mathbf{n}_e] (\psi - r_h \psi) ds \\
&\quad + \sum_{K \in \mathcal{M}_h} k_0^2 \langle \nabla \cdot (\varepsilon \mathbf{E}_h) - \varepsilon E_{3,h}, q - r_h q \rangle_K + \sum_{e \in \mathcal{B}_h(\Omega), e \notin \partial\Omega} k_0^2 \int_e ([\varepsilon \mathbf{E}_h] \cdot \mathbf{n}_e) (q - r_h q) ds
\end{aligned}$$

From (3.3)-(3.4), Lemma 3.2 and Lemma 3.3, we have for all $(\mathbf{V}, q) \in \mathbb{X}$,

$$|\mathbf{a}((\mathbf{e}, e_3), (\mathbf{V}, q))| \leq C_1 \left(\sum_{K \in \mathcal{M}_h} \eta_1(K)^2 \right)^{\frac{1}{2}} \|(\mathbf{V}, q)\|_{\mathbb{X}} + C_2 \left(\sum_{e \in \mathcal{B}_h(\Omega), e \notin \partial\Omega} \eta_1(e)^2 \right)^{\frac{1}{2}} \|(\mathbf{V}, q)\|_{\mathbb{X}},$$

where

$$\begin{aligned}
\eta_1(K)^2 &= h_K^2 (\|\mathbf{f} + k_0^2 \varepsilon \mathbf{E}_h + \nabla E_{3,h}\|_{[L^2(K)]^2}^2 + \|\nabla \cdot (\mathbf{f} + k_0^2 \varepsilon \mathbf{E}_h + \nabla E_{3,h})\|_{L^2(K)}^2 \\
&\quad + \|k_0^2 (\nabla \cdot (\varepsilon \mathbf{E}_h) - \varepsilon E_{3,h})\|_{L^2(K)}^2)
\end{aligned}$$

and

$$\eta_1(e)^2 = h_e (\|[\mathbf{f} + k_0^2 \varepsilon \mathbf{E}_h + \nabla E_{3,h}] \cdot \mathbf{n}_e\|_{L^2(e)}^2 + \|k_0^2 [\varepsilon \mathbf{E}_h] \cdot \mathbf{n}_e\|_{L^2(e)}^2)$$

and the constants C_1, C_2 depend only on the mesh shape-regularity.

Then, using the continuous inf-sup conditions for the bilinear form $\mathbf{a}(\cdot, \cdot)$, we have

$$\begin{aligned}
&\|\mathbf{E} - \mathbf{E}_h\|_{H(\mathbf{curl}, \Omega)} + \|E_3 - E_{3h}\|_{H^1(\Omega)} \\
&\leq \frac{1}{\alpha_1} \sup_{(\mathbf{V}, q) \in \mathbb{X}} \frac{|\mathbf{a}((\mathbf{e}, e_3), (\mathbf{V}, q))|}{\|(\mathbf{V}, q)\|_{\mathbb{X}}} \\
&\leq \frac{1}{\alpha_1} \sup_{(\mathbf{V}, q) \in \mathbb{X}} \frac{C_1 \left(\sum_{K \in \mathcal{M}_h} \eta_1(K)^2 \right)^{\frac{1}{2}} \|(\mathbf{V}, q)\|_{\mathbb{X}} + C_2 \left(\sum_{e \in \mathcal{B}_h(\Omega), e \notin \partial\Omega} \eta_1(e)^2 \right)^{\frac{1}{2}} \|(\mathbf{V}, q)\|_{\mathbb{X}}}{\|(\mathbf{V}, q)\|_{\mathbb{X}}} \\
&\leq C \left(\sum_{K \in \mathcal{M}_h} \eta(K)^2 \right)^{\frac{1}{2}},
\end{aligned}$$

where C depends only on the mesh shape-regularity, and

$$\eta(K)^2 = (\eta_1(K)^2 + \sum_{e \in \partial K, e \notin \partial\Omega} \eta_1(e)^2).$$

Using the technique of [3], we have the following lower bound estimate. The proof of this theorem is omitted here (for more details, see [22] Theorem 4.4).

Theorem 3.5. (Lower Bound) *Let $(\mathbf{E}, E_3) \in \mathbb{X}$, $(\mathbf{E}_h, E_{3,h}) \in \mathbb{X}_h$ be the solutions of problem (3.1) and problem (3.2). Then there is a constant $C_* > 0$, depending only on the mesh shape-regularity such that*

$$\eta(K) \leq C_* \{ (\|\mathbf{E} - \mathbf{E}_h\|_{H(\mathbf{curl}, \mathfrak{S}(K))} + \|E_3 - E_{3h}\|_{H^1(\mathfrak{S}(K))}) \}.$$

The above two theorems imply local efficiency of our adaptive finite element based on the a posteriori error estimate, since refining where the local indicators $\eta(K)$ are large is always necessary to reduce the error.

Here, we present the procedure ADAPTIVE which is based on a marking strategy due to E. Bänsch, P. Morin and R. H. Nochetto [2]. With the a posteriori error estimators (3.5), the

ADAPTIVE procedure of AIIFEA uses normal adaptive technique. From [20], we can get that (2.4) holds.

ADAPTIVE($\tilde{U}^*, \mathcal{M}^0, \epsilon^*$)

Choose parameters $0 < \Theta < 1$, set $i = 0$.

1. Compute the discrete solution $\tilde{U}^i \in \mathbb{X}^i$ over \mathcal{M}^i such that

$$\mathbf{F}(\tilde{U}^i, \mathbf{V}) = \mathbf{G}(\tilde{U}^*, \mathbf{V}), \quad \forall \mathbf{V} \in \mathbb{X}^i.$$
2. Compute the local indicators $\eta(K)$.
3. If $(\sum_{K \in \mathcal{M}^i} \eta(K)^2)^{\frac{1}{2}} \leq \epsilon^*$ return $(\tilde{U}^i, \mathcal{M}^i)$ to AIIFMA.
4. Mark a subset $\tilde{\mathcal{M}}^i \subset \mathcal{M}^i$ such that

$$\sum_{K \in \tilde{\mathcal{M}}^i} \eta(K)^2 \geq \Theta \sum_{K \in \mathcal{M}^i} \eta(K)^2.$$
5. Define $\widehat{\mathcal{M}}^i$ to be the set of all elements $K' \in \mathfrak{S}(K)$ for $K \in \tilde{\mathcal{M}}^i$.
6. Refine \mathcal{M}^i by using the longest edge refinement strategy over $K' \in \widehat{\mathcal{M}}^i$, get \mathcal{M}^{i+1} .
7. Set $i = i + 1$ and goto step (1).

4. Numerical Experiments

In this section we report several numerical examples to illustrate the performance of the method studied in this paper. In every numerical experiment, we solve the eigenvalue problem with the finite element inverse iteration algorithm over uniformly refined meshes and with the AIIFMA. Let N_j be the number of nodes of the j-th mesh, $E_{1,h} = |\lambda_h - \beta^2|$ the error of the minimum eigenvalue with the uniformly refined meshes, where λ_h is the approximate eigenvalue over the mesh of size h, and $E_{2,h} = |\lambda_j - \beta^2|$ the error with the adaptively refined meshes, where λ_j is the approximate eigenvalue of the j-th iteration. In the computations we used the PDE toolbox of MATLAB. The discrete algebraic eigenvalue problems are solved by the shifted inverse iteration algorithm with shift τ .

Example 1. This example is taken from [13] which concerns a rectangular dielectric waveguide with one ridge. The domain Ω is a rib domain like Figure 4, and we set $L = 12.7mm$, $H = 10.16mm$, $l = 2.54mm$, $h = 2.794mm$. Here, $\Omega = \Omega_1 \cup \Omega_2 \cup \Omega_3$ with $\epsilon_1 = 1.0$, $\epsilon_2 = 1.5$ and $\epsilon_3 = 1.0$.

Example (1.1): Let $k_0 = \omega \sqrt{\epsilon_0 \mu_0} \approx 0.78539816$ and $\tau = 0$. Figure 4 shows clearly that AIIFEA is better than the EIIA with the uniformly refined meshes, and the associated numerical

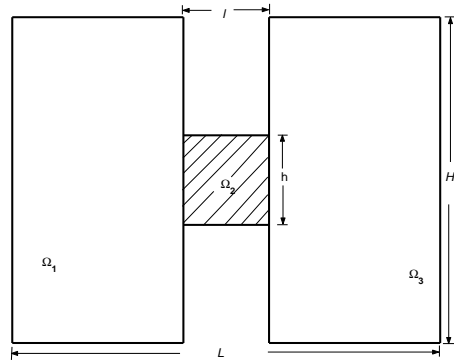


Fig. 4.1. Rectangular dielectric waveguide with one ridge

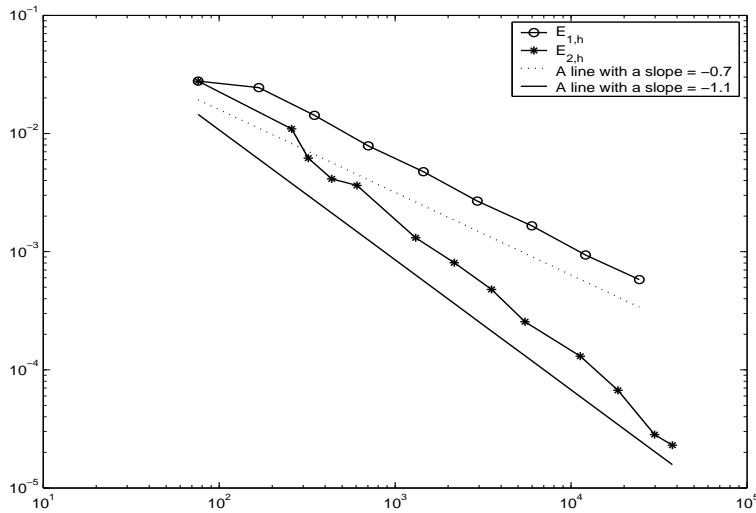


Fig. 4.2. Example 1.1: Performance of the error in terms of the number of nodes of the meshes

complexity is quasi-optimal: $|\lambda_j - \beta^2| \approx CN_j^{(-1.1)}$ is valid asymptotically. The performance of the quasi-optimal method is indicated by the line of slope -1.1. Figure 4.3 shows some adaptively refined meshes for this example.

Example (1.2): Let $k_0 \approx 0.80638829$ and $\tau = 0$. Figure 4 shows clearly that the associated numerical complexity is quasi-optimal: $|\lambda_j - \beta^2| \approx CN_j^{(-1.0)}$ is valid asymptotically.

Example (1.3): Let $k_0 \approx 0.80638829$, $\tau = 0.2$. Here, the analytical eigenvalue is $\beta_a^2 \approx 0.2171$. Figure 4 shows clearly the associated numerical complexity of AIIFEM is quasi-optimal: $|\lambda_j - \beta_a^2| \approx CN_j^{(-1.0)}$ is valid asymptotically.

Example 2. We consider an incomplete rectangular dielectric waveguide. This example is taken from [16]. The following Figure 4 shows the transverse domain of the waveguide material. $\Omega = [0, L] \times [0, H]$ with $H = 3mm$, $L = 9mm$, and $h_1 = 1.0mm$, $h_2 = 1.0mm$, $l_1 = 3.0mm$. In practical computation, we take $\varepsilon_1 = 3.58$ and $\varepsilon_2 = 1.0$.

Example (2.1): Let $k_0 = 1/3$ and $\tau = 0$. Figure 4 shows clearly that AIIFEA is better than the EIHA with the uniformly refined meshes, and the associated numerical complexity is quasi-optimal: $|\lambda_j - \beta^2| \approx CN_j^{(-1.0)}$ is valid asymptotically. The performance of the quasi-

optimal method is indicated by the line of slope -1.0. Figure 4.8 gives some adaptively refined meshes for this example.

Example (2.2): Let $k_0 = 4/15$, $\tau = 0$. Figure 4.8 shows clearly that the associated numerical complexity of AIIFEA is quasi-optimal: $|\lambda_j - \beta^2| \approx CN_j^{(-1.0)}$ is valid asymptotically.

Example (2.3): Let $k_0 = 1$, $\tau = 0$. Figure 4 shows clearly that the associated numerical complexity of AIIFEA is quasi-optimal: $|\lambda_j - \beta^2| \approx CN_j^{(-1.0)}$ is valid asymptotically.

Example 3. This example is taken from [10], where $\Omega = [0, L] \times [0, H]$ with $H = 0.6mm$ and $L = 1mm$. This waveguide is sketched in Figure 4, where $h_1 = 0.4mm$, $l_1 = 0.5mm$ and $\varepsilon_1 = 3.0$, $\varepsilon_2 = 1.0$.

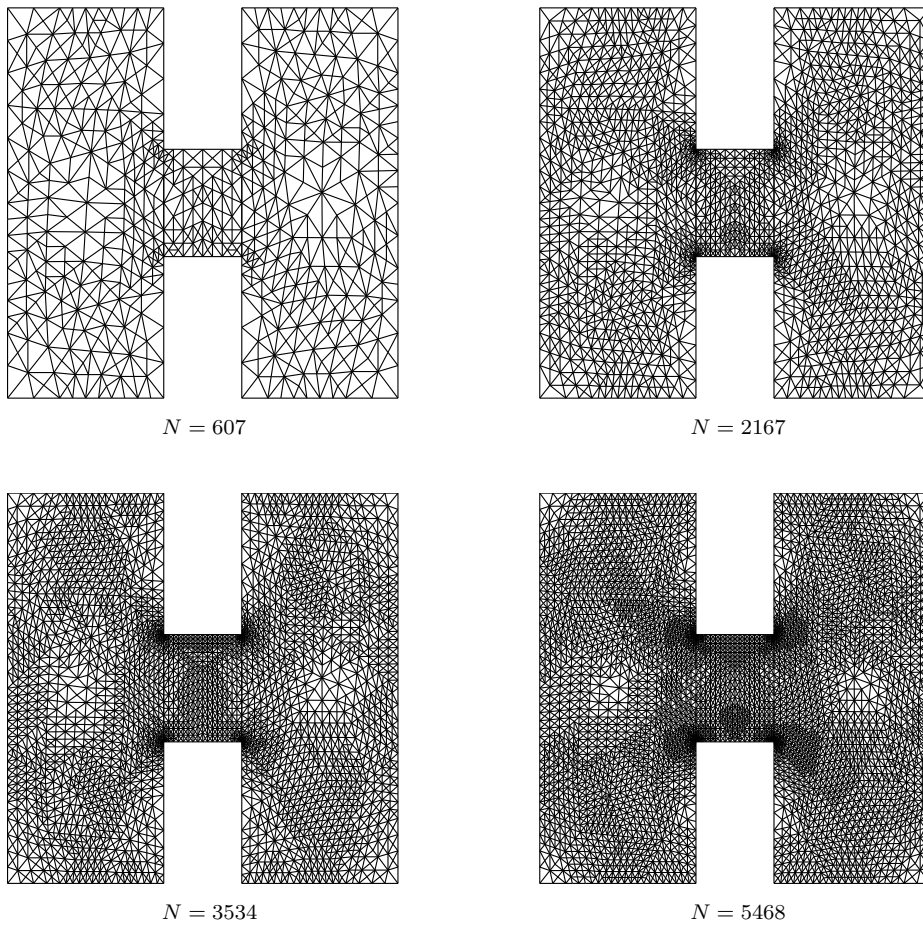


Fig. 4.3. The adaptively refined meshes for Example 1.1

Let $k_0 = 2.5$ and $\tau = 0$. Figure 4 shows clearly that AIIFEA is better than the EIIA with the uniformly refined meshes, and the associated numerical complexity is quasi-optimal: $|\lambda_j - \beta^2| \approx CN_j^{(-1.0)}$ is valid asymptotically. The performance of the quasi-optimal method is indicated by the line of slope -1.0. Figure 4.13 gives some meshes for this example.

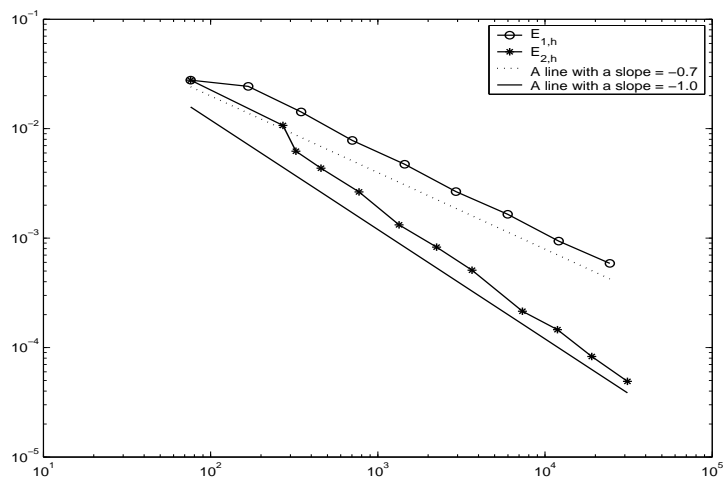


Fig. 4.4. Example 1.2: Performance of the error in terms of the number of nodes of the meshes

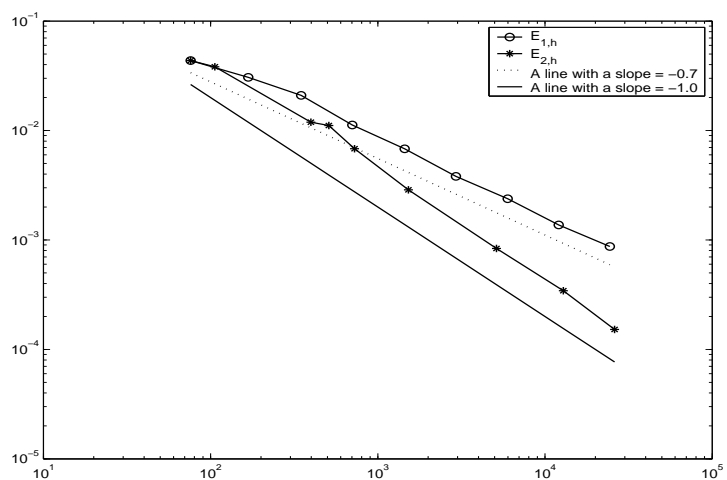


Fig. 4.5. Example 1.3: Performance of the error in terms of the number of nodes of the meshes

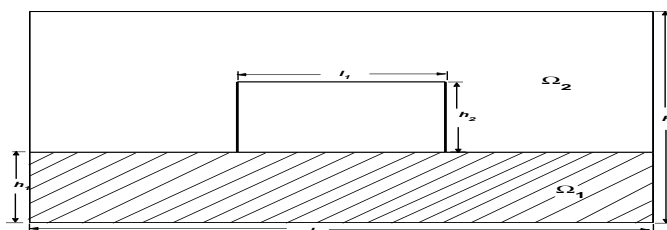


Fig. 4.6. Incomplete rectangular dielectric waveguide

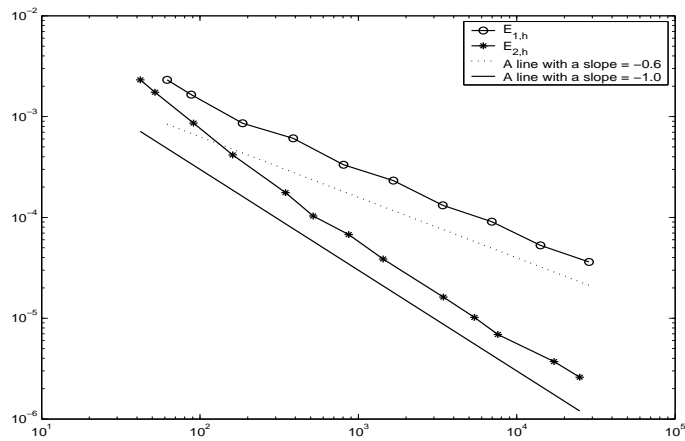


Fig. 4.7. Example 2.1: Performance of the error in terms of the number of nodes of the meshes

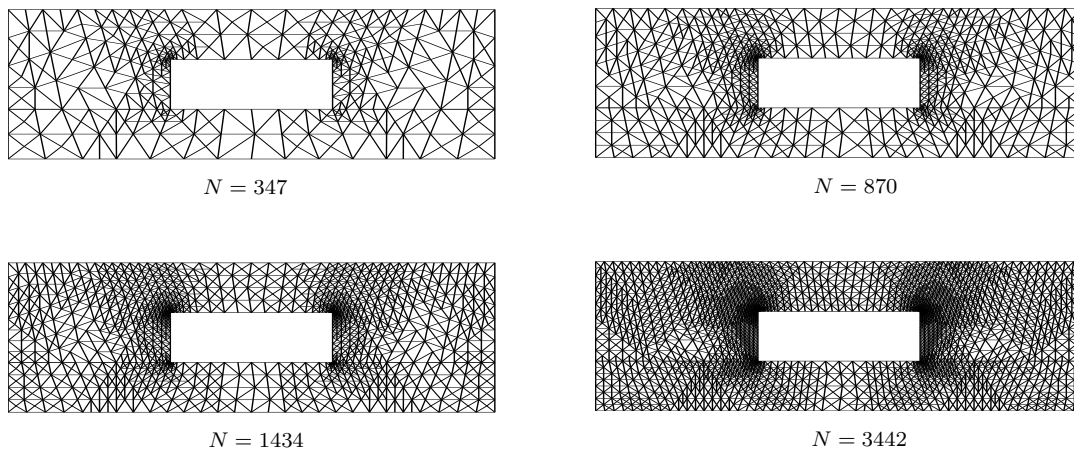


Fig. 4.8. The adaptively refined meshes for Example 2.1

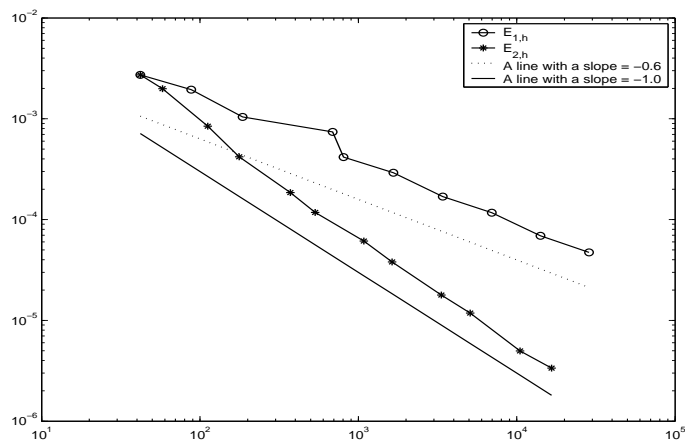


Fig. 4.9. Example 2.2: Performance of the error in terms of the number of nodes of the meshes

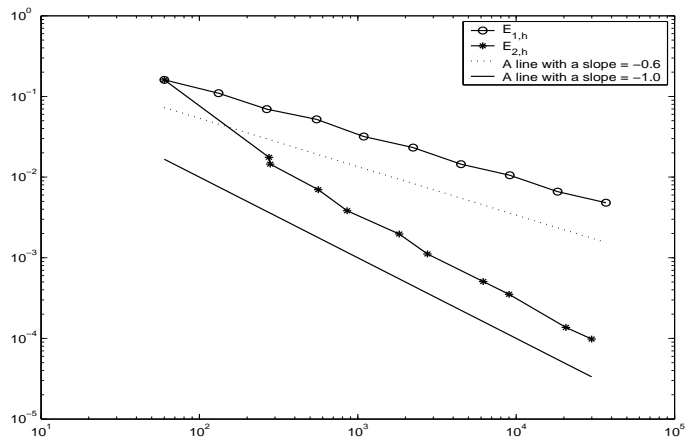


Fig. 4.10. Example 2.3: Performance of the error in terms of the number of nodes of the meshes

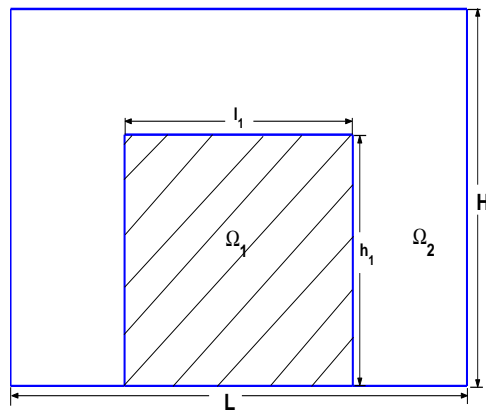


Fig. 4.11. Rectangular dielectric waveguide

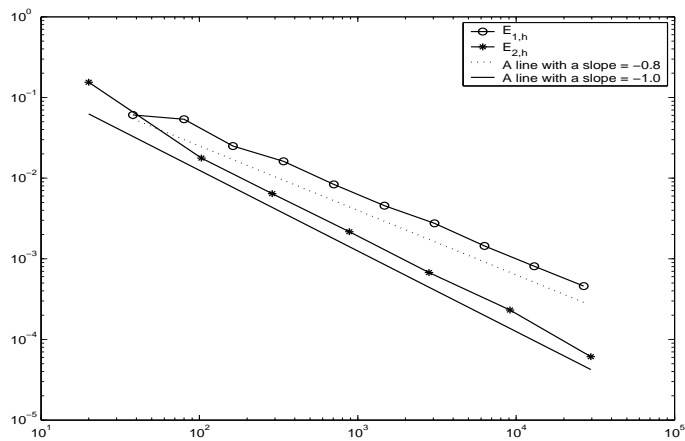


Fig. 4.12. Example 3: Performance of the error in terms of the number of nodes of the meshes

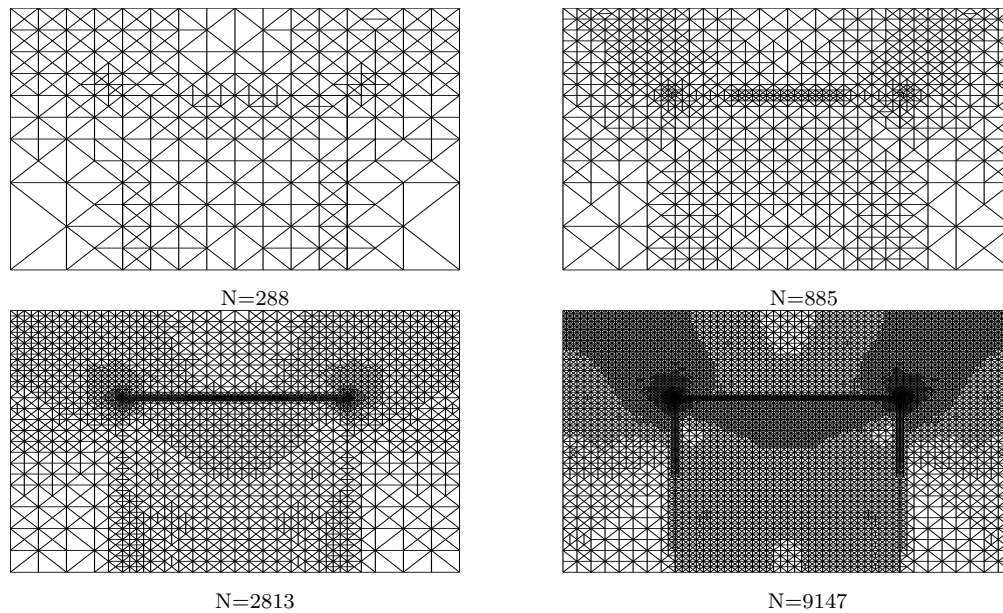


Fig. 4.13. The adaptively refined meshes for *Example 3*

Acknowledgments. I express my gratitude to Professor Zhiming Chen for his carefully reading of this paper and for his valuable comments and suggestions. I also thank the referees for their constructive comments and suggestions.

References

- [1] I. Babuška and J. Osborn, Eigenvalue Problems, in Handbook of Numerical Analysis, Elsevier-North Holland Amsterdam, 1991.
- [2] E. Bänsch, P. Morin and R. H. Nochetto, An adaptive Uzawa FEM for the Stokes problem convergence without the Inf-Sup condition, *SIAM J. Num. Anal.*, **40** (2002), 1207-1229.
- [3] R. Beck, R. Hiptmair, R.H.W. Hoppe, and B. Wohlmuth, Residual based a posteriori error estimators for eddy current computation, *ESAIM-Math. Model. Numer. Anal.*, **34** (2000), 159-182.
- [4] A. Bermúdez and D.G. Padreira, Mathematical analysis of a finite element method without spurious for computation of dielectric waveguides, *Numer. Math.*, **61** (1992), 39-57.
- [5] Z. Chen and S. Dai, On the efficiency of adaptive finite element methods for elliptic problems with discontinuous coefficients, *SIAM J. Sci. Comput.*, **24** (2002), 443-462.
- [6] Z. Chen and R.H. Nochetto, Residual type a posteriori error estimates for elliptic obstacle problems, *Numer. Math.*, **84** (2000), 527-548.
- [7] Z. Chen and J. Yuan, On finite element methods for inhomogeneous dielectric waveguides, *J. Comput. Math.*, **22** (2004), 188-199.
- [8] K.S. Chiang, Review of numerical and approximate methods for the modal analysis of general optical dielectric waveguide, *Optical and Quantum Electronics*, **26** (1994), 113-134.
- [9] P. Clément, Approximation by finite element functions using local regularization, *RAIRO Anal. Numer.*, **2** (1975), 77-84.
- [10] Z.J. Csendes and P. Silvester, Numerical solution of dielectric-loaded waveguide. I. finite-element analysis, *IEEE Trans, Microwave Theory Tech.*, **MTT-18** (1970), 1124-1131.
- [11] V. Girault and P.A. Raviart, Finite Element Methods for Navier-Stokes Equations, New York: North-Holland, Amsterdam, 1986.
- [12] R.F. Harrington, Time-Harmonic Electromagnetic Fields, New York: McGraw-Hill, 1961.

- [13] M. Israel and R. Miniowitz, Hermitian finite-element method for inhomogeneous waveguides, *IEEE Trans. Microwave Theory Tech.*, **MTT-38** (1990), 1319-1327.
- [14] J.M. Jin, *The Finite Element Methods in Electromagnetics*, New York: John Wiley & Sons, 1993.
- [15] P. Joly, C. Poirier, J.E. Roberts, and P. Trounev, A new nonconforming finite element method for the computation of electromagnetic guided waves I: mathematical analysis, *SIAM J. Numer. Anal.*, **33**:4 (1996), 1494-1525.
- [16] P. Lüsse, P. Stuwe, and H.-G. Unger, Analysis of vectorial mode fields in optical waveguides by a new finite difference method, *J. Lightwave Technology*, **12**:3 (1994), 487-493.
- [17] P. Monk, *Finite Element Methods for Maxwell's Equations*, Oxford University Press, 2003.
- [18] J.C. Nédélec, Mixed finite elements in \mathbb{R}^3 , *Numer. Math.*, **35** (1980), 315-341.
- [19] L. Vardapetyan and L. Demkowicz, Full-wave analysis of dielectric waveguides at a given frequency, *Math. Comp.*, **72**:241 (2002), 105-129.
- [20] R. Verfürth, *A Review of A Posteriori Error Estimation and Adaptive Mesh-Refinement Techniques*, New York: Wiley-Teubner, 1996.
- [21] L. Wang, Z. Chen, and W. Zheng, An adaptive multilevel method for time-harmonic maxwell equations with singularities, submitted to *SIAM J. Sci. Comput.*.
- [22] J. Yuan, *Finite Element Method for the Inhomogeneous Dielectric Waveguides*, Ph.D. Thesis, AMSS, Beijing, 2005.
- [23] J. Zhou, Analysis of finite element approximation for time-dependent maxwell problems, *Math. Comp.*, **73** (2004), 1089-1105.